

# A PFG-NMR Study of Restricted Diffusion in Heterogeneous Polymer Particles

John Georg Seland,<sup>\*,1</sup> Matteo Ottaviani,<sup>†</sup> and Bjørn Hafskjold<sup>\*</sup>

<sup>\*</sup>Department of Chemistry, Norwegian University of Science and Technology, N-7491 Trondheim, Norway;  
and <sup>†</sup>Department of Physical Chemistry, University of Padova, 35131 Padova, Italy

E-mail: johinsel@chembio.ntnu.no; matteo@pcf.chembio.ntnu.no; bhaf@chembio.ntnu.no.

Received October 4, 2000; accepted March 15, 2001

**The diffusion resistance to monomers during heterogeneous polymerization of polyolefin particles may have a significant effect on the observed activity. This diffusivity is, in general, unknown. To gain more information on this diffusion resistance in such systems, PFG-NMR has been used to measure the diffusion of organic solvents in various systems of porous polymer particles. In such systems the complex morphology and geometry demands careful analysis of the PFG-NMR attenuation curve. In this study, effects from restricted diffusion, domains having different diffusivity, and internal magnetic field gradients are expected. Thus, the obtained diffusivities have to be considered carefully, and a way to analyze the data taking these effects into account is presented.** © 2001 Academic Press

**Key Words:** PFG-NMR; restricted diffusion; polymer particles; internal magnetic field gradients; tortuosity.

## INTRODUCTION

The influence of restricting geometry on the measured diffusivity is of great importance in different kinds of porous media, like porous rocks, biological systems, and polymer systems. In a pulsed field gradient nuclear magnetic resonance (PFG-NMR) experiment, the observation time can be varied from a few milliseconds up to several seconds. Because of effects from the restricting geometry, the measured self-diffusion coefficient,  $D(t)$ , depends on the observation time,  $t_d$ , and is sensitive to physical parameters like permeability and the volume fraction of the diffusing species.  $D(t)$  can be related to certain characteristics of the porous medium such as the surface-to-volume ratio and the tortuosity (1–5). Taking into account only geometrical restrictions of the medium,  $D(t)$  of a diffusing fluid is found to decrease with observation time and reach a plateau value, which represents the tortuosity,  $\mathcal{T}$ , of the system (1–3).

During a heterogeneous polymerization of polyolefins the original catalyst particles fracture and are encapsulated in solid polymer. Porous polymer particles are made, and they grow as the polymerization proceeds (6, 7). The diffusion resistance to

monomers during polymerization to polyolefin particles may have a significant effect on the observed activity. This diffusion resistance depends on the diffusivity of the monomers in the different areas of the particles, and this diffusivity is, in general, unknown (7, 8).

The purpose of this article is to show how PFG-NMR can be used to measure diffusion of small molecules in porous polymer particles and to discover which effects one has to take into consideration to give reliable values for the diffusion coefficient in different areas of the particles.

The PFG-NMR method has been used to measure diffusion coefficients of liquids in different areas of such a system. Measurements done in polyethylene (PE) particles produced in a full-scale industrial reactor are compared with measurements done in model systems consisting of monodisperse porous polystyrene particles having various pore size distributions.

In heterogeneous systems, internal magnetic field gradients may be a significant source of error. These internal gradients are induced because of differences in magnetic susceptibility between the different areas in an heterogeneous sample and may consist of a broad distribution of values with both polarities (9–11). A coupling between the applied and internal magnetic field gradients will occur (12), and depending on the relative strength between the internal gradients and the applied ones, the measured diffusion coefficient may not correspond to the actual diffusivity in the system.

This source of error can often be eliminated by introducing bipolar gradients in the pulse sequence (13–17), but in a recent publication (18), it was shown that when bipolar gradients are used to suppress the effects of internal gradients, the observation time must be kept to a level where the square root of mean square displacement does not exceed the distance in which it is likely that an internal gradient will change its polarity or its strength significantly. This has to be taken into account at long observation times in some of the systems studied here, and we discuss how this error can be compensated for.

The PE particles have a complex morphology and geometry. When a liquid is added to this system, it will occupy different domains of the particles. The two main domains will be the

<sup>1</sup> To whom correspondence should be addressed.

semicrystalline phase of the polymer and that in the cavities inside the porous particle. In addition, there is a distribution of pore sizes, which will, because of restricted diffusion, have different influences on the measured diffusivity. Thus, the attenuation curve has to be analyzed carefully, and it is important to have control of the effects which influence this curve.

In this study effects of internal magnetic field gradients, different diffusion domains, and restricted diffusion are analyzed carefully, and we suggest the most convenient and correct way of analyzing the obtained attenuation curves.

## THEORY

Generally, in a pulsed field gradient (PFG) experiment, the echo attenuation for an ensemble of molecules undergoing free Brownian motion is given by

$$\ln \frac{I}{I_0} = -\gamma^2 \delta^2 g_e^2 D t_d, \quad [1]$$

where  $\gamma$  is the gyromagnetic ratio,  $g_e$  is the effective applied magnetic field gradient,  $\delta$  is the effective length of the applied gradient pulse,  $D$  is the self-diffusion coefficient, and  $t_d$  is the effective observation time. The parameters  $g_e$  and  $t_d$  will depend on the type of PFG sequence used.

When working with heterogeneous media, it is convenient to define the so-called reciprocal lattice wave vector,  $q = \gamma g_e \delta / 2\pi$ , which describes the reciprocal space of the restricting geometry in the system.

To reduce the effects of internal magnetic field gradients, we made use of the pulse sequences with pairs of bipolar gradients as shown in Figs. 1b and 1c.

In (18) it was shown that if the square root of the mean square displacement during the observation time exceeds the distance in which it is likely that an internal gradient will change its polarity or its strength significantly, the use of bipolar gradients may fail to suppress effects of internal magnetic field gradients. With long observation time, this has to be taken into account in some of the measurements performed in this study.

In the systems studied here, it is also important to take into consideration the effects of domains having different diffusivities, effects of restricted diffusion, and the influence these effects have on the measurements performed.

There are various equations describing the effects of several diffusion domains. In the limit of slow exchange between the different domains, the process is described by

$$\frac{I}{I_0} = \sum_{i=1}^n p_i e^{-4\pi^2 q^2 D_i t_d}, \quad [2]$$

where  $D_i$  is the diffusion coefficient describing the diffusion of the fractions of molecules,  $p_i$  in domain  $i$  of the system, and the other symbols are as described in the previous equations. Equation [2] does not take into account relaxation effects. If the relaxation times are significantly different for the different

domains, each fraction ( $p_i$ ) will be a function of the different time intervals in the pulse sequence used in the experiment.

In the limit of fast exchange the attenuation is described by an average diffusion coefficient

$$D_{av} = \sum_{i=1}^n p_i D_i. \quad [3]$$

The attenuation is then mono-exponential and is given by

$$\ln \frac{I}{I_0} = -4\pi^2 q^2 D_{av} t_d. \quad [4]$$

Again, no effects of differences in relaxation times are taken into consideration.

Between the two limits mentioned above, one has to consider different degrees of exchange between the various domains during the observation time.

Restricted diffusion has different influences on the measurements. As the diffusion time increases, more molecules will be influenced by the restricting boundaries, giving a lower value of the measured diffusion coefficient. Thus, the measured diffusion coefficient will be time dependent.

The diffusion behavior in the limit of long (infinite) observation time, when the heterogeneity of the porous system is probed, may be described by the tortuosity,  $\mathcal{T}$ , defined as

$$\frac{D_\infty}{D_0} = \frac{1}{\mathcal{T}}, \quad [5]$$

where  $D_0$  is the value of the diffusion coefficient at  $t = 0$ , i.e., the value for bulk diffusion of the liquid, and  $D_\infty$  is the corresponding value at  $t = \infty$ .

If a large fraction of the molecules are influenced by the restrictions during the observation time, or during the gradient pulse, the diffusion propagator may no longer be Gaussian. The attenuation may be influenced by different degrees of restricted diffusion, and by higher order terms of the gradient strength ( $g_e^4$ ), giving a nonlinear attenuation, concaved upward (19).

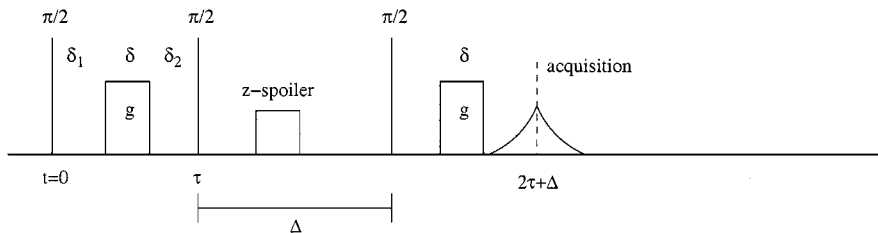
If the square root of the mean square displacement during the gradient pulse,  $r_\delta = \sqrt{2D\delta}$ , is relatively small compared to the size of the spacing between the restricting barriers, only a small fraction of the molecules will be influenced by the barriers. Then, the diffusion propagator will be Gaussian to the first order in  $g^2$  if  $qa \ll 1$  (20), where  $a$  is the spacing between the restricting barriers in the system. Thus, at low values of the gradient strength (low  $q$  values) the influence from higher order terms of  $g$  is low, and the effective diffusion coefficient is given by (19)

$$\lim_{q \rightarrow 0} \frac{\partial \ln(I/I_0)}{\partial q^2} = -4\pi^2 D_{eff}(t_d) t_d \quad [6]$$

and can be found from the initial slope of the attenuation curve. This is known as the ‘‘second cumulant approximation’’ (19).

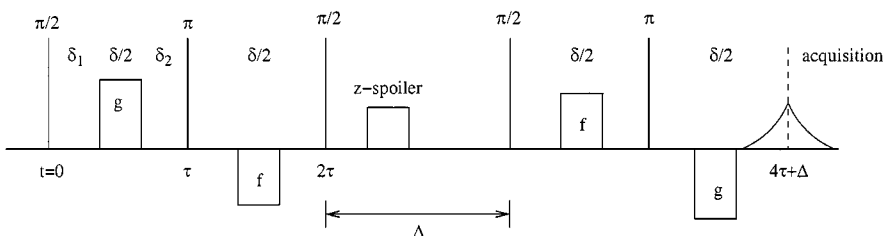
On the other hand, if  $r_\delta$  is much longer than spacing between the restricting boundaries ( $qa \gg 1$ ), all of the molecules in the

(a)



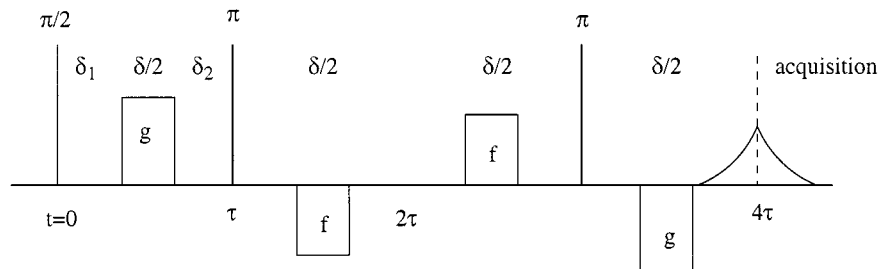
$$\ln \frac{I}{I_0} = -\gamma^2 \delta^2 g^2 D \left( \Delta + \tau - \frac{\delta}{3} \right)$$

(b)



$$\ln \frac{I}{I_0} = -\gamma^2 \delta^2 \left[ g - \frac{1}{2}(g - f) \left( \frac{\Delta + \tau - \frac{\delta}{6}}{\Delta + \frac{3}{2}\tau - \frac{\delta}{6}} \right) \right]^2 D \left( \Delta + \frac{3}{2}\tau - \frac{\delta}{6} \right)$$

(c)



$$\ln \frac{I}{I_0} = -\gamma^2 \delta^2 \left[ g - \frac{1}{2}(g - f) \left( \frac{\tau - \frac{\delta}{6}}{\frac{3}{2}\tau - \frac{\delta}{6}} \right) \right]^2 D \left( \frac{3}{2}\tau - \frac{\delta}{6} \right)$$

**FIG. 1.** Pulse sequences used in the diffusion experiments: (a) the pulsed field gradient stimulated echo sequence (12); (b) the 13 intervals bipolar PFG stimulated echo sequence (16); (c) the 11 intervals bipolar PFG spin echo sequence (17).  $f$  and  $g$  are the strengths of the applied gradients. The effective gradients and the observation times are as given in the expressions for the attenuations. The time intervals are as described in the figures.

ensemble will be influenced by the boundaries. Random diffusion causes the phase distribution of the spins to be Gaussian during the gradient pulse, even though the displacements are not Gaussian (21). The diffusion propagator will then also be Gaussian. This is usually called a “quasi-homogeneous” system.

In the case where  $r_\delta$  is equal to the spacing between the restricting boundaries, one cannot use the second cumulant

approximation, and the system cannot be considered to be quasi-homogeneous. It is then complicated to extract the true diffusion coefficient in the porous system, and it is only possible if the geometry of the system is simple and well defined.

Internal magnetic field gradients, several diffusion domains, and restricted diffusion are all effects which have to be taken into consideration in the measurements presented here.

## MATERIALS AND METHODS

The PE particles were delivered from Borealis A/S where they were produced in a full-scale slurry phase reactor. The grain sizes of the particles studied were 250–500  $\mu\text{m}$  in diameter.

Pore size distribution of the particles was determined by use of mercury intrusion with a Pascal 140 instrument, and the porosity was determined by use of a Micrometric AccuPyc 1330 Helium-pycnometer, and with the Pascal 140 instrument. Scanning electron microscopy (SEM) pictures of both the outer surface of the particles and of sliced particles were obtained. A razor blade was used for slicing the particles.

Toluene and methanol were separately added to the PE particles. The purpose was to have liquids with different solubilities in the amorphous phase of PE, thus making it possible to vary the ratio between the amount of liquid in the semi-crystalline phase of PE and in the cavities inside the particles.

NMR samples of the PE particles were prepared by filling the particles in a 5-mm NMR tube. Toluene or methanol was then added in excess to the tubes. The samples were dried at 40°C until it was observed visually that the interparticle liquid had evaporated; the remaining liquid is then to be found inside the particles. The tubes were then sealed off.

In addition to the samples of PE particles, some samples of liquid added to monosized polystyrene particles were investigated. Three different types of polystyrene particles were studied. One system consisted of totally compact polystyrene spheres with a mean diameter of 20  $\mu\text{m}$  (sample PS1) and was delivered from Duke Scientific (U.S.A). The other two systems were porous particles with a mean diameter of 15  $\mu\text{m}$  and with different interior pore size distributions (samples PS2 and PS3). These particles were produced at SINTEF Applied Chemistry in Trondheim, Norway.

The polystyrene particles were filled in the NMR tubes and were then totally immersed in liquid so that both the internal cavities and the cavities between the particles were occupied by liquid. Distilled water was added to sample PS1, while toluene was added to samples PS2 and PS3.

Diffusion experiments were performed on a Bruker Avance DMX200 instrument (magnetic field strength = 4.7 T, resonance frequency for protons = 200.13 MHz) using a commercial diffusion probe from Bruker (PH MIC 200 WB 1H SAT 5/10). An applied gradient strength in the range 0–600 G/cm was used. Unless stated otherwise, the experiments were performed at 25.0  $\pm$  0.5°C.

The pulse sequences given in Fig. 1 were used. In each diffusion experiment the different time intervals were kept constant, while the strength of the gradients was varied. The length of the gradient pulse ( $\delta$ ) was 0.5 ms in the experiments performed with the monopolar PFGSTE sequence (Fig. 1a). In the experiments performed with bipolar sequences (Figs. 1b and 1c), the length of the gradient pulse ( $\delta/2$ ) was 0.5 ms.

To minimize the cross terms between applied and internal gradients, all the diffusion experiments were performed with  $\delta_1 = \delta_2$ , and to dephase, and thus eliminate the signal from solid

semi-crystalline PE at the time of the echo, a value of  $\delta_1 = \delta_2 \geq 0.5$  ms was used.

The applied gradient strength was calibrated by performing diffusion experiments in distilled water slightly doped with  $\text{CuSO}_4$ , and in dried glycerol, for calibration at high gradient strength (22).

## RESULTS AND DISCUSSION

### SEM Analysis and Porosity Measurements

The scanning electron microscopy (SEM) pictures of the PE particle are shown in Fig. 2. The particles have a very irregular

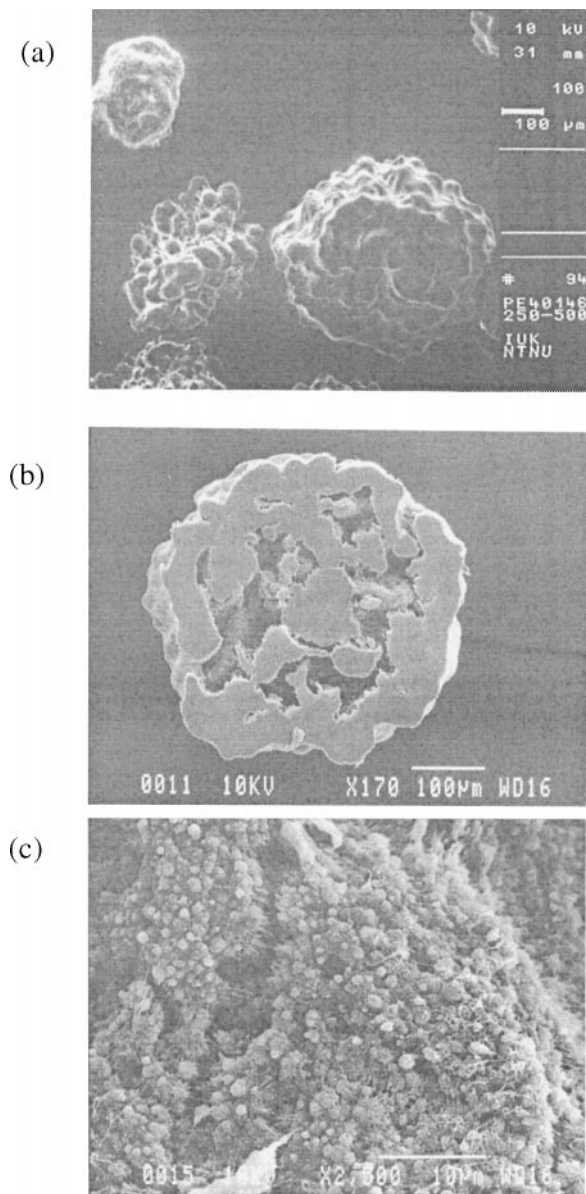


**FIG. 2.** Scanning electron microscopy (SEM) pictures of the PE particle. Unsliced particles (a), a sliced particle (b), and a magnified area of the interior surface of a cavity (c).

surface, indicating a rather complex structure and geometry. The picture of a sliced particle (Fig. 2b) shows that the interior of the particles consists of rather large cavities, with a diameter of 20–60  $\mu\text{m}$ . The interior surface of these cavities seems to be made up of smaller grains (Fig. 2c). Because the sliced surface is smeared out, it is impossible to obtain any information on the interior geometry in these areas of the particles based on the SEM pictures.

The size distribution of the pores to be found inside the particles, shown in Fig. 3a, is very broad. The mean pore radius is around 0.5–1.0  $\mu\text{m}$ , but there are pores varying from about 100 nm up to a few micrometers. The porosity of the particles was measured to be 8%.

Comparing the pore size distributions with the SEM pictures of the PE particles, it seems like the larger cavities are not accounted for in the mercury porosity measurements. This is probably because some of these larger cavities are isolated and therefore will not contribute in the porosity measurements. In addition, the largest cavities inside the particles are of the same size as the cavities expected to be found between the particles when they are closely packed. To avoid contribution from the interfering cavities between the particles, the mercury intrusion measurements did not detect pores/cavities larger than around 5  $\mu\text{m}$ .

Therefore, based on the SEM pictures, and on the arguments mentioned above, one may conclude that the porosity is

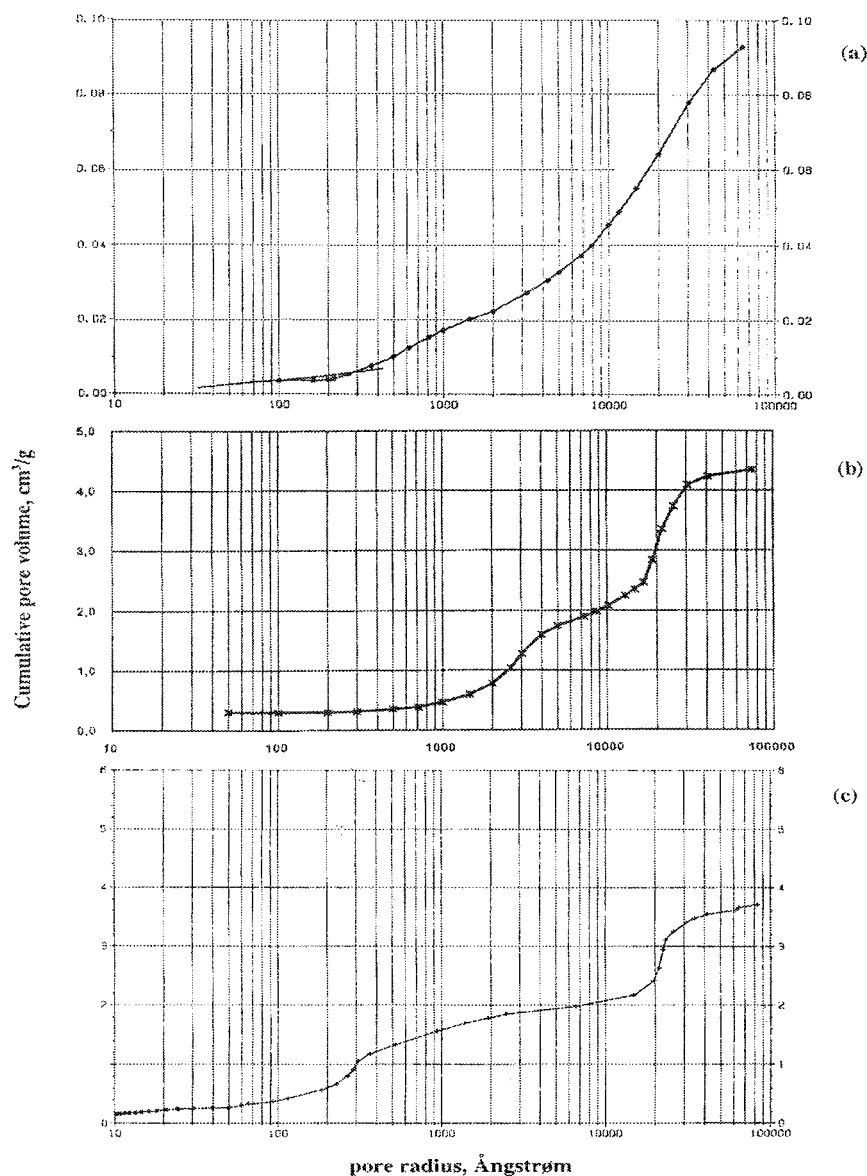


**FIG. 3.** Pore size distributions of the PE particles (a), polystyrene particles PS2 (b), and polystyrene particles PS3 (c). The pore radius, [Å] is plotted as a function of the cumulative pore volume [cm<sup>3</sup>/g].

higher than the value given by the porosity measurements. The interior of the particles can be divided into two main domains, the large cavities, 20–60  $\mu\text{m}$  in diameter, and the areas consisting of semi-crystalline polymer, where smaller pores, ranging from a few  $\mu\text{m}$  down to about 100 nm, are found.

The pore size distributions of the porous polystyrene particles are shown in Figs. 3b and 3c. These distributions are much more discrete than the one found in the PE particles. In sample PS2 the mean pore radius of the internal pores is around 0.2–0.5  $\mu\text{m}$ , while for the PS3 sample it is around 0.02–0.03  $\mu\text{m}$ . The radii of the cavities between the particles are 2–3  $\mu\text{m}$  in both samples.

### Diffusion in the Polystyrene Systems

The idea behind studying the systems of polystyrene particles immersed in a liquid is that the geometry of these systems is better defined than that in the system of liquid-filled PE particles. By doing diffusion experiments in the polystyrene systems, it is possible to have a better understanding of, and to interpret, what processes are taking place in the system of PE particles.

The FFT spectrum (not shown) of the samples of polystyrene spheres immersed in liquid has a bandwidth at half height of around 30 Hz, indicating that the internal magnetic field gradients are low in these samples (9). No significant difference in the measured diffusion coefficients was found using a monopolar compared to a bipolar pulse sequence, so for these samples all the experiments were performed using the monopolar PFGSTE sequence (Fig. 1a).

Before analyzing the results from the diffusion measurements in the polystyrene samples, it is important to describe the expected effects from restricting geometry and different diffusion domains in these systems. The length of the gradient pulse,  $\delta$ , was 0.5 ms. This gives a value of around 1  $\mu\text{m}$  for the square root of mean square displacement  $r_\delta$  during the gradient pulse for the molecules diffusing in the porous system.

For sample PS1, water is found only between the compact particles. The cavities between the particles are 8–10  $\mu\text{m}$  in diameter, and the second cumulant approximation is valid. The initial slope of the attenuation curve represents the value of the effective diffusion coefficient.

In samples PS2 and PS3, toluene is found both in the cavities between the particles and in the cavities inside the particles. In addition, one may expect some of the toluene to dissolve in the polymer matrix, but as shown later, the diffusion experiments indicated that this fraction does not contribute significantly to the total signal. It was therefore disregarded in further analysis. The cavities between the particles are 5–6  $\mu\text{m}$  in diameter, so the second cumulant approximation is valid here.

The internal pores in sample PS2 are around 0.5–1.0  $\mu\text{m}$  in diameter, so for this area Eq. [6] may be invalid. However, considering the total ensemble of molecules in this sample, one may assume a smaller fraction of the molecules to be influenced by the walls during the gradient pulse, and the second cumulant approximation may be applied, if the value of  $q$  is kept sufficiently low (20). In sample PS3 the internal pores are much smaller

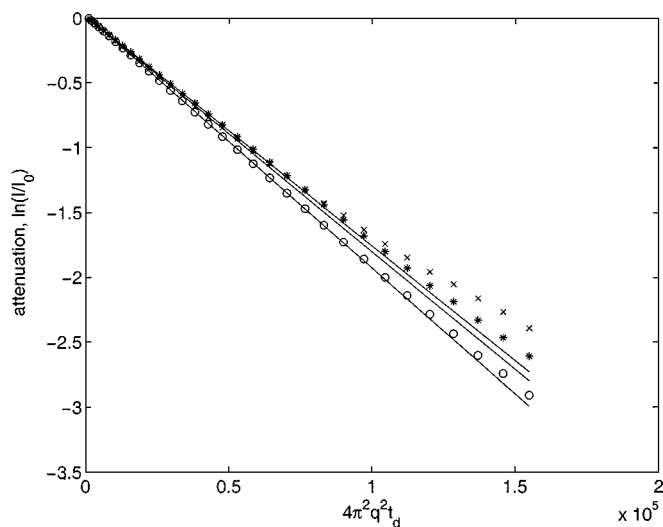


**FIG. 4.** Obtained attenuations from diffusion experiments performed in the polystyrene samples, PS1 (+), PS2 (o), and PS3 (\*). The PFGSTE sequence (Fig. 1a) was used in all of the experiments. The value of  $\Delta$  is 8 ms. The solid lines are linear fits of Eq. [6] to the initial slope of the curves.

than  $r_\delta$ , so the interior of these particles may be considered as a “quasi-homogeneous” system. The attenuation curve will therefore consist of mean values of signals from two different areas, the quasi-homogeneous internal system, and the external system where the second cumulant approximation is valid.

The attenuations obtained from the PFGSTE experiments in the polystyrene samples are shown in Fig. 4. The observed concave attenuation curves obtained for the polystyrene samples may be caused by the effect of domains having different diffusivities and/or by restricted diffusion. One can expect the diffusivity of the liquid to be found in the cavities inside the particles to be lower than that in the cavities between the particles. However, it is impossible to separate these two fractions from each other because of the effect of restricted diffusion and because the difference in diffusivity is too low. There will also be a total exchange between the small and large pores, even during the shortest observation time.

In addition, since the shape of the curve is the same for all the polystyrene samples, and we know that in sample PS1 there is a single value of the diffusion coefficient, one cannot justify the use of a multicomponent fit in samples PS2 and PS3.

The system is therefore most correctly described according to Eq. [4], using the initial slope of the attenuation (Eq. [6]) as the average, effective diffusion coefficient. In all of the polystyrene samples the attenuation is linear down to at least  $-0.7$ , showing that the second cumulant approximation is valid (19, 20).

The obtained effective diffusion coefficients in the polystyrene samples are shown in Fig. 5, where the normalized diffusion coefficient,  $D(t)/D_0$ , is plotted as a function of the observation time  $t_d$ .

In the system of compact polystyrene spheres immersed in distilled water (sample PS1), the obtained tortuosity value,  $\mathcal{T}$ , is as expected in a system of random loose packing of monosized

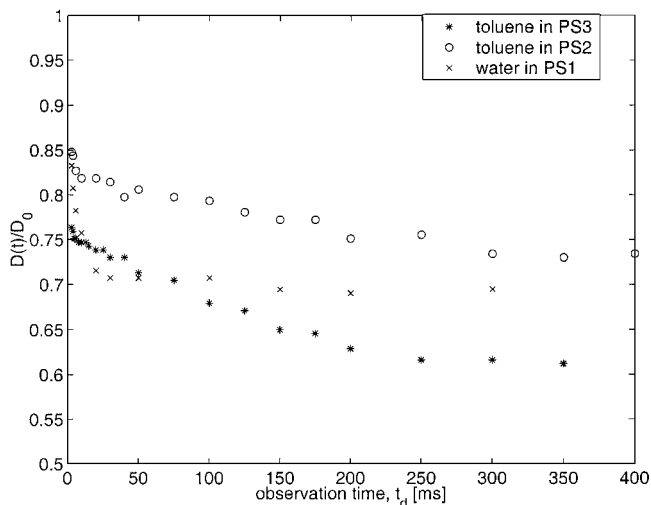


**FIG. 5.** Diffusion measurements in the samples of monosized polystyrene particles. The normalized diffusion coefficient,  $D(t)/D_0$ , as a function of the observation time,  $t_d$ . The PFGSTE sequence was used in all of the experiments. The bulk values of the diffusion coefficients were  $2.28 \times 10^{-9}$  and  $2.30 \times 10^{-9} \text{ m}^2 \text{ s}^{-1}$  for toluene and distilled water, respectively.

spheres (1, 18). Sample PS2 has a slightly lower tortuosity value than sample PS1, and longer observation time is necessary to reach the tortuosity limit. This is as expected because of the presence of the rather large interior cavities in sample PS2, which function as an additional diffusion path through the particles. In sample PS3, on the other hand, the situation is different. Here, the internal cavities are so small that they will strongly restrict the diffusion inside the particles, and the tortuosity limit is higher in this sample.

These results show that the effective diffusivity is influenced by the different sizes of the pores in the system, and that in a system like this, consisting of a mixture of large and small pores, one cannot justify a separation of diffusion in small and large pores, based on the multiexponential model (Eq. [2]). The most correct approach is to use the initial slope of the attenuation curve as a measure of the effective time-dependent diffusion coefficient,  $D(t)$ , in the system.

### Diffusion in the Polyethylene Systems

In the systems of porous PE particles the geometry is complex. Because of the broad distribution of pore sizes, the diffusing molecules will be affected by the geometry to different degrees, depending on which area of the particle they occupy. In addition, a significant amount of the liquid will dissolve in the semi-crystalline phase of PE.

Organic liquids have different solubilities in the semi-crystalline phase of PE. In this study we have used toluene and methanol as added liquids. The solubility of toluene is higher than that of methanol. The idea is that the liquid with highest solubility in semi-crystalline PE will have the highest possibility of being found in the smallest cavities of the particle. By variation of the amount and type of liquid added, cavities of different

sizes are filled up. The diffusivity in the different areas of the particle can then be determined.

Three samples with different amounts of added toluene, and three samples with different amounts of added methanol, were studied. For toluene, the amounts added were 0.25, 0.17, and  $0.10 \text{ cm}^3/\text{g PE}$ , while for methanol the amounts added were 0.24, 0.15, and  $0.10 \text{ cm}^3/\text{g PE}$ .

The FFT spectra obtained in the diffusion experiments of the sample with  $0.25 \text{ cm}^3$  of toluene/g of PE are shown in Fig. 6. At a low value of the applied gradient strength, two broad, partially overlapping bands are visible.

As the gradient strength increases, the band at higher frequency decays faster than the other one. At sufficiently high gradient strengths, the signal from toluene inside the cavities has totally dephased, and the remaining signal is from the toluene which is dissolved in the semi-crystalline phase of PE.

The bandwidth at half height in Fig. 6 (upper) is around 400–500 Hz, indicating that significant internal gradients may be present in these sample. Further analysis showed that the monopolar PFGSTE pulse sequence gave a significantly lower diffusivity compared to a bipolar pulse sequence, so the bipolar pulse sequences were used in the diffusion experiments performed in these systems.

The diffusion measurements performed on the porous PE particles, using a bipolar sequence, resulted in a nonlinear attenuation curve, concaved upward. It is reasonable to assume that the nonlinear attenuation is mainly caused by the effect of the two main diffusion domains in the system and that the broad peaks in Fig. 6 (upper) are a superposition of signals from liquid in semi-crystalline PE and in the cavities, which cannot be separated in the spectrum.

Thus, at relatively small values of  $t_d$  (slow exchange), one may expect the attenuation to be described by Eq. [2] for

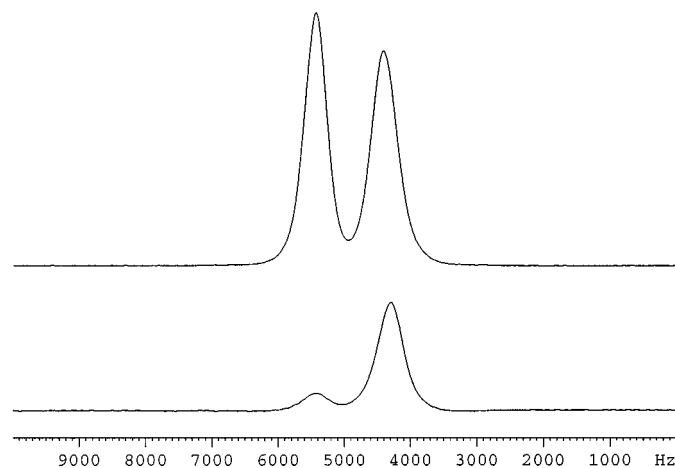


**FIG. 6.** FFT spectra obtained from diffusion experiments in the samples of PE particles with toluene added, at a low value of the applied gradient strength (upper spectrum) and at a high value of the applied gradient strength (lower spectrum). The 11-intervals bipolar pulse sequence was applied in this diffusion experiment.

diffusion of liquid in semi-crystalline PE and in cavities of different sizes. Since a typical value for diffusion of liquid dissolved in semi-crystalline PE is around  $1\text{--}5 \times 10^{-11} \text{ m}^2 \text{ s}^{-1}$  (23, 24), even at  $t_d \approx 200 \text{ ms}$ , the diffusion length in this domain will be approximately  $2\text{--}3 \text{ }\mu\text{m}$ , and there should be no significant amount of exchange between the two domains. In addition, as shown below, it was found that the estimated fraction of liquid found in semi-crystalline PE did not vary significantly with the observation time, which should be the case if there was significant exchange taking place. Another indication of exchange is that, in the case of a significant degree of exchange, the diffusion coefficient for liquid dissolved in semi-crystalline PE should increase with increasing observation time, which was not observed.

However, one should be careful when interpreting multiexponential decay curves. In the system studied here there are effects of restricted diffusion contributing to the curvature of the attenuation. This effect is not taken into account using Eq. [2]. In addition, the measurements performed in the systems of polystyrene spheres showed that because of fast exchange one could not justify a separation of signals from molecules diffusing in pores having a diameter around  $0.05 \text{ }\mu\text{m}$  compared to pores with a diameter of  $5\text{--}10 \text{ }\mu\text{m}$ , using a sum of exponentials. It is therefore difficult to verify if there are two or three different diffusivities in the PE systems or how much of the concave in the obtained attenuation is caused by restricted diffusion in the cavities during the gradient pulse.

Instead of doing a multiexponential fit of the total attenuation curve, one may use the fact that, at sufficiently high attenuations, the signal from the faster diffusing liquid in the cavities does not contribute to the observed signal. A linear fit to the last part of the attenuation curve that represents the diffusion of liquid in the semi-crystalline phase of PE may then be performed. The intercept at  $q = 0$  represents the fraction of this signal. The obtained linear model can then be subtracted from the total experimental attenuation, and the resulting curve then represents diffusion of liquid in the cavities of different sizes.

In Fig. 7 the results of making a linear fit to the last part of the curve, followed by subtracting this model from the total curve, are shown. The resulting curve is not linear. This can be explained by taking into account the effect of restricted diffusion during the gradient pulse, which will result in a nonlinear attenuation similar to what was observed in the experiments performed in the systems of polystyrene spheres. One can then use the second cumulant approximation and make a linear fit to the initial part of this curve.

To have as good control of the different effects as possible, this is, in our opinion, the correct method for analyzing attenuation curves from systems having a broad distribution of pore sizes, like the PE particles.

Because of the broad pore size distribution in these systems, one cannot *a priori* expect that the second cumulant approximation can be applied for the molecules diffusing in the cavities

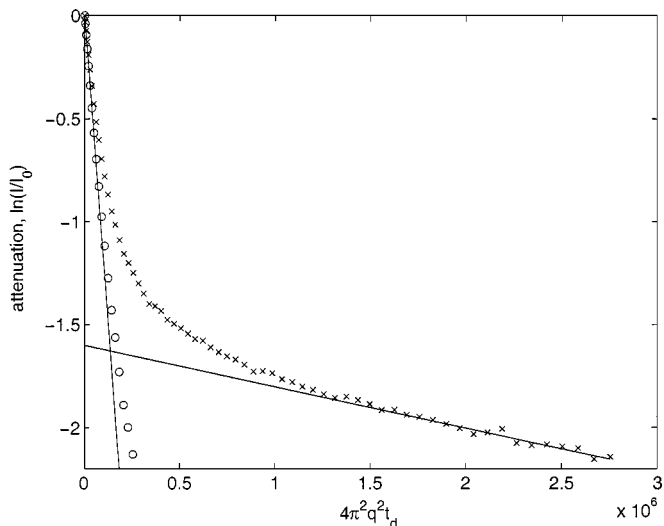


**FIG. 7.** Obtained attenuation in a PFG (bipolar 13 intervals) experiment in a sample of PE particles with toluene added.  $t_d = 8.7 \text{ ms}$ . Obtained experimental data ( $\times$ ) and the curve fitted to the signal from toluene dissolved in semi-crystalline PE. This curve is subtracted from the experimental points, and the initial slope of the resulting curve, ( $\circ$ ), is determined, representing diffusion in the cavities of the particles.

(20). Since the attenuation is linear down to at least  $-0.5$ , we assume it to be valid, though it should be mentioned that, in the sample having the lowest filling of toluene, the linearity of the initial slope was poor, indicating effects of restricted diffusion in small cavities.

The diffusion experiments performed in the samples with different amounts of liquid added showed that the normalized diffusion coefficients representing diffusion in the cavities ( $D_{cav}$ ) vary with both type and amount of liquid added and with the observation time. Because the rather low amount of liquid found in the semi-crystalline PE, the signal-to-noise ratio was rather poor for the part of the experimental attenuation curve representing this diffusivity. The diffusion coefficient representing diffusion of liquid in semi-crystalline PE ( $D_{sc}$ ) varied randomly in the range  $1\text{--}4 \times 10^{-11} \text{ m}^2 \text{ s}^{-1}$ , a value which corresponds to similar results found in the literature (23, 24).

Though the variation in the obtained  $D_{sc}$ 's was random, there was a tendency to obtain higher values at short observation time, indicating effects of restricted diffusion. Since the main interest in this study is the diffusivity in the cavities, the values from the semi-crystalline domains are not given here.

At long observation times, it was found that the diffusion coefficient representing diffusion of liquid in the cavities depended on the  $\tau$ -value in the pulse sequence. As the  $\tau$ -value decreases, the value of  $D_{cav}(t)$  increases. Such a dependency was not found at short observation times. Thus, as showed in (18) the use of bipolar gradients does not totally suppress the cross term between applied and internal gradients at longer observation times, and this has to be taken into consideration in the measurements performed.

**TABLE 1**  
**Results from the Diffusion Experiments in the Samples**  
**of PE Particles**

	Toluene added			Methanol added		
$(\text{cm}^3/\text{g})_{\text{tot}}$	0.25	0.17	0.10	0.24	0.15	0.10
$p_{\text{sc}}$	0.2	0.4	0.7	0.05	0.15	0.2
$(\text{cm}^3/\text{g})_{\text{sc}}$	0.05	0.07	0.07	0.01	0.02	0.02
$(\text{cm}^3/\text{g})_{\text{cav}}$	0.20	0.10	0.03	0.23	0.13	0.08
$T$	2.1	2.1	3.0	2.0	2.0	2.5

*Note.* The total amounts of toluene and methanol added,  $(\text{cm}^3/\text{g})_{\text{tot}}$  are given.  $p_{\text{sc}}$  is the fraction of liquid found in the semi-crystalline PE, determined from the model fit of the last part of the experimental attenuations. The estimated amounts of liquid in semi-crystalline PE,  $(\text{cm}^3/\text{g})_{\text{sc}}$ , and in the cavities,  $(\text{cm}^3/\text{g})_{\text{cav}}$ , is given for each sample. The tortuosity values,  $T$ , determined from the diffusivity limit at long observation time is given with an uncertainty of  $\pm 0.15$ .

To compensate for the unsuppressed cross term in the attenuations at long observation time, we tried to measure the diffusion coefficient as a function of  $\tau$  at fixed (long) observation time, as done in (18). We found that this resulted in unrealistic high values when extrapolating to  $\tau = 0$ . The quality of the data from the measurements of the  $\tau$ -dependency at long observation time does not justify the use of this approach. We therefore choose to use the result obtained at the lowest possible  $\tau$ -value as a lower limit for the value of  $D_{\text{cav}}(t)$  at long observation time.

From the fractions of liquid dissolved in semi-crystalline PE,  $p_{\text{sc}}$ , it is possible to estimate the amount of liquid to be found in semi-crystalline PE, and the amount to be found in the cavities, for each sample. All the important parameters determined are summed up in Table 1. The relative amount of liquid dissolved in semi-crystalline PE is approximately constant in each type of sample with different filling degree. Clearly, the solubility of methanol is lower than toluene.

Relaxation measurements performed indicated that the value of  $T_1$  for both liquid in semi-crystalline PE and in the cavities is around 0.6–1 s. It was found that the fraction of signal from liquid in semi-crystalline PE did not vary significantly with the observation time. As mentioned above, this indicates that exchange of liquid between semi-crystalline PE and the cavities is not significant.

It was also observed that  $p_{\text{sc}}$  varied with the value of  $\tau$  in the pulse sequence. This time interval is influenced by transverse relaxation. As the  $\tau$  value increases,  $p_{\text{sc}}$  increases, showing that the  $T_2^*$  value for the liquid in the semi-crystalline phase of PE is longer than that for the liquid in the cavities. This is in correspondence with what is observed in the FT spectra from the diffusion experiments. At long  $\tau$ -values (around 15–20 ms) the FT spectrum at low values of the gradient strength is similar to the spectrum obtained at high gradient strength but low value of  $\tau$  (Fig. 6b). At high values of  $\tau$ , one is therefore left with the signal from the liquid in semi-crystalline PE. This is also in correspondence with relaxation measurements, which indicated that the  $T_2^*$  value for one of the domains are significantly shorter than the other. Thus, the  $T_2^*$  value for liquid in the cavities is shorter than that for liquid dissolved in the semi-crystalline PE.

This may be explained by the effects from diffusion in internal magnetic field gradients contributing to the total dephasing of the transverse magnetization.

The results obtained for the time-dependent diffusivity in the cavities of the PE particles in the different samples studied are given in Fig. 8.

For the samples with toluene added, there is no significant difference for the results obtained in the two samples having the highest filling and the tortuosity limit obtained is the same. For the sample having the lowest filling ( $0.10 \text{ cm}^3/\text{g}$ ) there is a significant difference. Already at the shortest observation time, the tortuosity limit is reached, and the tortuosity value is significantly higher than that in the other samples. As indicated by the estimated amount of liquid found in the cavities in this sample, only the smallest cavities are filled up. In the other two samples

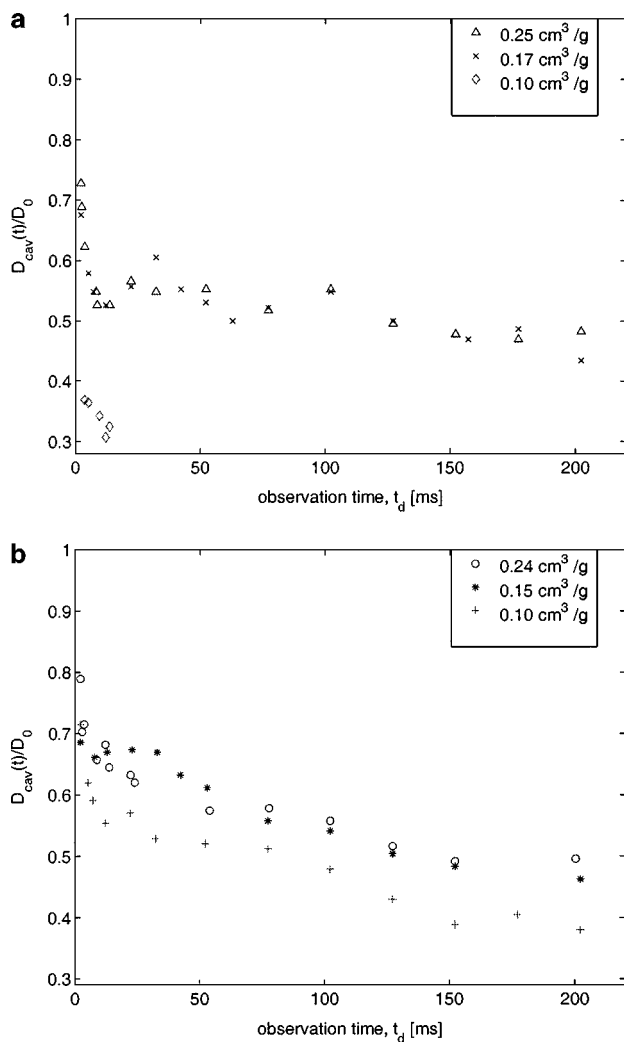


**FIG. 8.** Diffusion measurements in the samples where toluene (a) and methanol (b) were added to the PE particles. The normalized diffusion coefficient in the cavities,  $D_{\text{cav}}(t)/D_0$ , as a function of the observation time. The bipolar sequences (Figs. 1b and 1c) were used in all of the experiments. The bulk values used for the liquids were  $2.28 \times 10^{-9}$  and  $2.42 \times 10^{-9} \text{ m}^2 \text{ s}^{-1}$  for toluene and methanol, respectively (22).

both small and larger cavities are more or less completely filled. This explains the difference in the obtained tortuosity values for these samples.

In the samples with methanol added, the two samples having the highest filling have about the same tortuosity limit as the corresponding samples with toluene, and we may assume that here both the small and large pores are filled, which is also indicated by the estimated amount of liquid found in the cavities given in Table 1. In the sample with lowest filling the tortuosity value is higher, but not as high as that in the corresponding sample with toluene. As indicated in Table 1, when the same amount of toluene and methanol is added separately to the PE particles, a higher fraction of toluene dissolves in semi-crystalline PE, while in the sample with methanol a fraction of the larger cavities will be filled up in addition to the small cavities. This explains the difference in the time-dependent diffusivity for these two samples and the difference in tortuosity value obtained.

The results presented in Table 1 show that the effective diffusivity, and thus the estimated tortuosities, vary with the filling degree of the different cavity sizes.

## CONCLUSIONS

We have shown how PFG-NMR can be used to measure diffusion in different systems of porous polymer particles. Diffusion measurements performed in samples of randomly packed monosized porous and nonporous polystyrene particles show that because of restricted diffusion and exchange, one cannot separate diffusion in small and large pores using a multiexponential model. The most correct approach in these samples is to use the initial slope as a measure of the effective diffusion coefficient in the system, according to the second cumulant approximation.

This has to be taken into consideration when the measurements in the system of PE particles are interpreted. We show that by subtracting the signal from diffusion and liquid dissolved in semi-crystalline PE, it is possible to use the second cumulant approximation to determine the diffusivity of the liquid to be found in the cavities of the particles. By variation of the amount of liquid added, cavities of different sizes are occupied, and the tortuosity value,  $T$ , in the different areas of the particles can be determined.

It was also shown that the use of bipolar gradients in the pulse sequence do not completely suppress the influence of internal gradients at longer observation times. The unsuppressed cross

term between the internal and applied magnetic field gradients depends on the value of  $\tau$  is the pulse sequence used, and it is important to keep this value as low as possible in the experiments performed. Clearly, the diffusion coefficients, and thus the tortuosity, vary with the filling degree of the cavities in the PE particles.

## ACKNOWLEDGMENTS

We gratefully acknowledge financial support from The Research Council of Norway (NFR) through the Polymer Science Program. We would also like to thank Dr. G. H. Sørland for valuable and interesting discussions during this work.

## REFERENCES

1. Latour, L. L., Kleinberg, R. L., Mitra, P. P., and Sotak, C. H., *J. Magn. Reson. A* **112**, 83 (1995).
2. Latour, L. L., Mitra, P. P., Kleinberg, R. L., and Sotak, C. H., *J. Magn. Reson. A* **101**, 342 (1993).
3. Latour, L. L., Svoboda, K., Mitra, P. P., and Sotak, C. H., *Proc. Natl. Acad. Sci.* **91**, 1229 (1994).
4. Mitra, P. P., Sen, P. N., and Schwartz, L. M., *Phys. Rev. B* **47**, 8565 (1993).
5. Hürlimann, M. D., Helmer, K. G., Latour, L. L., and Sotak, C. H., *J. Magn. Reson. A* **11**, 169 (1994).
6. Zacca, J. J., Debling, J. A., and Ray, W. H., *Chem. Eng. Sci.* **51**, 4859 (1996).
7. Hutchinson, R. A., Chen, C. M., and Ray, W. H., *J. Appl. Polym. Sci.* **44**, 1389 (1992).
8. McKenna, T. F., Dupuy, J., and Spitz, R., *J. Appl. Polym. Sci.* **63**, 315 (1997).
9. Drain, L. E., *Proc. Phys. Soc.* **80**, 1380 (1962).
10. Zhong, J., Kennan, R. P., and Gore, J. C., *J. Magn. Reson.* **95**, 267 (1991).
11. Hürlimann, M. D., *J. Magn. Reson.* **131**, 232 (1998).
12. Tanner, J. E., *J. Chem. Phys.* **52**, 2523 (1970).
13. Karlicek, R. F., and Lowe, I. J., *J. Magn. Reson.* **37**, 74 (1980).
14. Latour, L. L., Li, L., and Sotak, C. H., *J. Magn. Reson. B* **101**, 72 (1993).
15. Cotts, R. M., Hoch, M. J. R., Sun, T., and Markert, J. T., *J. Magn. Reson.* **83**, 252 (1989).
16. Sørland, G. H., Hafskjöld, B., and Herstad, O., *J. Magn. Reson.* **124**, 172 (1997).
17. Sørland, G. H., Aksnes, D., and Gjerdåker, L., *J. Magn. Reson.* **137**, 397 (1999).
18. Seland, J. G., Sørland, G. H., Zick, K., and Hafskjöld, B., *J. Magn. Reson.* **146**, 14 (2000).
19. Mitra, P. P., and Halperin, B. I., *J. Magn. Reson. A* **113**, 94 (1995).
20. Wang, L. Z., Caprihan, A., and Fukushima, E., *J. Magn. Reson. A* **117**, 209 (1995).
21. Neumann, C. H., *J. Chem. Phys.* **60**, 4508 (1974).
22. Holz, M., and Weingartner, H., *J. Magn. Reson.* **92**, 115 (1991).
23. Fleischer, G., *Colloid Polym. Sci.* **262**, 919 (1984).
24. Fleischer, G., *Polym. Commun.* **26**, 20 (1985).